VERTEBRATE BIOLOGY

REVISTA DE Biología Tropical

https://doi.org/10.15517/zn2j2m47

Embryogenesis and early larval development of the fish *Pimelodus grosskopfii* (Siluriformes: Pimelodidae)

Yanan S. Ortiz-Acevedo[1]; https://orcid.org/0000-0002-6322-2917
Andrés J. Bonilla-Reyes[1]; https://orcid.org/0000-0002-6218-2925
Luisa Fernanda Londoño-Ramírez[1]; https://orcid.org/0000-0002-5387-0689
Gersson Vásquez-Machado[2]; https://orcid.org/0000-0002-4737-7038
Ana Lucía Estrada-Posada[3]; https://orcid.org/0000-0003-3585-3719
Jonny Andrés Yepes-Blandón[1]*; https://orcid.org/0000-0001-6276-5488

1. Grupo de Investigación en Organismos Acuáticos Nativos y Exóticos (GIOANE), Instituto de Biología, Universidad de Antioquia, Medellín, Colombia; yanansamarao@gmail.com, andresjulian.bonilla@udea.edu.co, luisa.londonor@udea.edu.co, jonny.yepes@udea.edu.co (*Correspondence)
2. Diagnóstico Veterinario HISTOLAB, Carrera 5A No. 1-62, 250001, Chía, Cundinamarca, Colombia; gmvasquezm@unal.edu.co
3. ISAGEN S.A. E.S.P, Medellín, Antioquia, Colombia; aestrada@isagen.com.co

Received 27-VIII-2025. Corrected 12-XI-2025. Accepted 26-II-2026.

ABSTRACT

Introduction: Despite its ecological importance, a detailed characterization of the embryonic and early larval development is lacking for the neotropical siluriform *Pimelodus grosskopfii*.
Objective: To describe the ontogenetic and larval development of *P. grosskopfii*.
Methods: Key ontogenetic events were documented from fertilization through 20 days post-hatching using optical microscopy, histology, and scanning electron microscopy at 28.4 °C.
Results: Embryonic development proceeded through six distinct stages (zygote, cleavage, blastula, gastrula, segmentation, and organogenesis) and was completed in 11.6 hours, notably faster than other neotropical siluriforms. Newly hatched larvae (4.6 ± 0.5 mm total length) develop from telolecithal eggs with meroblastic cleavage restricted to the animal pole. Histological analyses revealed accelerated organogenesis with barbel rudiments appearing by 13 hours post-hatching and specialized sensory corpuscles by 17.5 hours. The transition to endogenous feeding occurred at 17.5 hours post-hatching, with complete yolk sac absorption by 31 hours. By day nine, larvae developed multiple dental rows (30-40 teeth per row), and by day 14, histological sections revealed complete mandibular ossification and advanced development of olfactory rosettes, gill structures, and the digestive tract.
Conclusion: This chronological sequence of morphological and histological changes provides a developmental framework for comparative studies among catfishes and contributes to understanding evolutionary patterns in teleost ontogeny.

Key words: catfish; histology; ontogeny; larvae; embryonic development.

RESUMEN

Embriogénesis y desarrollo larval del pez *Pimelodus grosskopfii* (Siluriformes: Pimelodidae)

Introducción: A pesar de su importancia ecológica, el siluriforme neotropical *Pimelodus grosskopfii* carece de una caracterización detallada de su desarrollo embrionario y larvario temprano.

Objetivo: Describir el desarrollo ontogenético y larval de *P. grosskopfii*.
Métodos: Los eventos ontogenéticos clave se documentaron desde la fertilización hasta los 20 días posteriores a la eclosión utilizando microscopía óptica, histología y microscopía electrónica de barrido a 28.4 °C.
Resultados: El desarrollo embrionario pasó por seis etapas distintas (cigoto, clivaje, blástula, gástrula, segmentación y organogénesis) y se completó en 11.6 horas, notablemente más rápido que otros siluriformes neotropicales. Las larvas recién eclosionadas (4.6 ± 0.5 mm de longitud total) se desarrollan de huevos telolecíticos con segmentación meroblástica restringida al polo animal. Los análisis histológicos revelaron una organogénesis acelerada, con la aparición de rudimentos de barbillas a las 13 horas tras la eclosión y corpúsculos sensoriales especializados a las 17.5 horas. La transición a la alimentación endógena se produjo a las 17.5 horas tras la eclosión, con una absorción completa del saco vitelino a las 31 horas. A los nueve días, las larvas desarrollaron múltiples filas dentales (30-40 dientes por fila) y, a los 14 días, los cortes histológicos revelaron una osificación mandibular completa y un desarrollo avanzado de rosetas olfativas, estructuras branquiales y el tracto digestivo.
Conclusiones: Esta secuencia cronológica de cambios morfológicos e histológicos proporciona un marco de desarrollo para estudios comparativos entre bagres y contribuye a la comprensión de los patrones evolutivos en la ontogenia de los teleósteos.

Palabras clave: bagre; histología; ontogenia; larvas; desarrollo embrionario.

INTRODUCTION

The catfish *Pimelodus grosskopfii* (Steindachner, 1879), commonly known as "Capaz" or "Barbudo," is an endemic species of the Magdalena-Cauca Basin, Colombia (Mojica et al., 2006; Ortega-Lara et al., 2006; Villa-Navarro et al., 2017) of significant socioeconomic importance for the riparian communities (Maldonado-Ocampo et al., 2005). However, its populations face an uncertain future due to a severe decline in wild individuals, driven by multiple threats (Mojica et al., 2012). The primary factors contributing to this decline include habitat degradation caused by pollution, channel modifications for agriculture, sedimentation, and unregulated fishing, all of which pose significant risks to the species (González et al., 2014). Estimates suggest that the species has declined by 90 % (Villa-Navarro et al., 2016). As a result, it was classified as Vulnerable (A2d) in the Red Book of Freshwater Fishes of Colombia (Lasso et al., 2011; Mojica et al., 2012). This designation signifies a suspected population reduction of at least 30% over a ten-year period or three generations, primarily attributed to actual or potential levels of exploitation (Criterion d). Due to the continued severity of these declines, the species was further reclassified as Critically Endangered (Villa-Navarro et al., 2016). The decline in fishing has economic, social, and ecological consequences. This situation highlights the urgent need to develop and implement strategies to mitigate these threats, support population recovery, and ensure the sustainable use of this commercially important species (Cala Cala, 2019; Observatorio Español de Acuicultura [OESA], 2018).

Among the methodologies for maintaining and restoring fishery resources, restocking is a key strategy. This approach involves releasing captive-bred individuals into the wild to replenish and increase population numbers within a specific geographic area. However, its successful implementation requires scientific knowledge of the species' fundamental biology to ensure survival in natural environments (Puley & Charles, 2022).

In the captive rearing of freshwater species for restocking programs, larviculture aims to secure high survival rates across various developmental stages. This is achieved by implementing management and nutritional strategies that foster the consistent production of high-quality juveniles in controlled environments (Castro-Ruiz et al., 2019). Despite its importance, large-scale larviculture remains a critical bottleneck in fish production, often marked by high mortality rates. These losses are attributed to factors such as cannibalism (Atencio-García

& Zaniboni-Filho, 2006; Ramirez-Merlano et al., 2010) and poor acceptance of inert diets, which stem from insufficient knowledge and improper management during the initial feeding period (Atencio et al., 2010; Zadmajid et al., 2019). This challenge is compounded by a limited understanding of key developmental events necessary for the maturation of vital systems—including the sensory, digestive, and locomotor systems—that are crucial for survival (Prieto & Atencio, 2008). Therefore, a thorough understanding of the timeline of these early developmental processes is essential for designing effective management and feeding protocols, thus guaranteeing stable and continuous juvenile output in aquaculture systems (Rønnestad et al., 2013).

Regarding early ontogeny and larval development, authors such as Zavala-Leal et al. (2011) and Portella et al. (2014) emphasize the importance of studying these processes in fish across various fields. These studies aim to describe anatomical, physiological, behavioral, and ecological changes that occur over short periods. Such processes occur in all species at specific rates and exhibit considerable variation among individuals within the same family (Rønnestad et al., 2013). Furthermore, they are closely related to the fish's life stage, influencing the refinement of instincts and enhancing larval survival in natural environments.

On the other hand, most of the available literature on organogenesis and larval development in fish focuses on commercially important species, such as *Prochilodus magdalenae* (Arias-Gallo et al., 2010; Yepes-Blandón et al., 2022), *Piaractus brachypomus* (Collazos-Lasso et al., 2014; Díaz-Olarte et al., 2010), and *Eremophilus mutisii* (Moncaleano et al., 2018), among others. In the case of *P. grosskopfii*, although some studies exist on embryonic development (Valbuena-Villarreal et al., 2012), gaps remain in the understanding of the development of structures involved in key vital functions of larvae, such as food detection and capture, respiration, locomotion, predator tracking, and escape behavior.

Therefore, it is essential to assess the early ontogenetic development of *P. grosskopfii*, including the development of various organ systems (sensory, digestive, and musculoskeletal) that will enable the individual to acquire the anatomical and physiological characteristics necessary for survival upon release into the environment. This approach will enhance the scientific understanding of the species, thereby support the improvement of its captive production and contribute to conservation programs.

MATERIALS AND METHODS

Ethics Statement: All procedures involving animal handling were conducted according to the Guide for the Care and Use of Laboratory Animals (Albus, 2012). The National Aquaculture and Fisheries Authority (AUNAP) of Colombia authorized the study under Resolutions 0955 of 2020 and 0071 of 2025.

Study area: This study was conducted at Piscícola San Silvestre S.A., located in Barrancabermeja, Santander, Colombia, at kilometer 7 on the road to the El Llanito district (07°06'30.8" N & 73°51'22.7" W). The farm is situated at an altitude of 74 m. a. s. l., within a tropical humid forest zone, according to Holdridge and Tosi Jr. (1967). The average annual temperature is 28.2 °C, with a relative humidity of 75 %.

Biological material: Samples were obtained from the induced spawning of eight female (mean weight: 350 g) and 17 male (267.35 g) *P. grosskopfii*. This broodstock was sourced from various locations along the Magdalena River and had been acclimated to captive conditions for one year prior to the study. Individuals were selected based on sex and external reproductive traits. Females exhibited a swollen abdomen with reddened and dilated urogenital papillae, while males released milt upon abdominal stripping. Female reproductive maturity was further confirmed via ovarian biopsy, assessing for germinal vesicle migration and oocyte diameter (Vazzoler, 1996).

Following selection, the fish were segregated by sex and transferred to two rectangular concrete tanks (2.3 m^3) for an 8-hour period before the reproduction protocol was initiated.

Hormonal induction: A combination protocol was utilized. Females were treated with carp pituitary extract (CPE) at a total dose of 4 mg/kg of body weight (11.2 mg in total), administered in two injections: an initial priming dose of 10 % (1.12 mg) and a resolving dose of 90 % (10.08 mg) given 12 hours later. The CPE was diluted in saline solution at a concentration of 1 mL/g of body weight (totaling 5.6 ml for the eight females, with an average of 0.7 ml per injection). Males received a single dose of a gonadotropin releasing hormone (GnRH) analogue combined with domperidone at 0.5 ml/kg of live weight. This different treatment for males was intended to increase milt volume, following the findings of Riveros-Pinilla et al. (2017). The dose was administered four hours after the females' first CPE application. Throughout the induction period in the holding tanks, water quality parameters were as follows: temperature ranged from 27.5 to 29.5 °C, pH was 8.02, and dissolved oxygen (DO) was 11.04 mg/L.

Gamete collection and harvesting: From the total number of induced specimens, one female and three males were randomly selected for gamete extraction, achieving a 3 : 1 male-to-female ratio, followed by in vitro fertilization. The gametes were mixed and activated by adding a 5 % sodium bicarbonate ($NaHCO_3$) solution for 5 min, gently stirring with a pipette. The mixture was then washed with running water to remove the residual solution, and this process continued for 30 min, with regular water changes and sampling every 5 min to assess the fertilization rate (70 % after one hour). Temperature was recorded hourly using a multiparameter device (YSI Pro Series), from fertilization until hatching.

The fertilized eggs were subsequently transferred to a 60 L upward-flow incubator, with a water flow rate of 4 L/min, to initiate the incubation process. Fertilized eggs (n = 20) were collected at each stage—early (zygote, cleavage, and gastrula) and late (segmentation to hatching)—according to the time intervals outlined in Table 1. The samples were photographed using an optical microscope to monitor and describe developmental changes. Embryogenesis was divided into six stages based on established reference points for freshwater fish, such as *Danio rerio* (Kimmel et al., 1995) and *Capoeta trutta* (Zadmajid et al., 2017): zygote, cleavage, blastula, gastrula, segmentation, and organogenesis.

The hatched larvae were transferred to a 2.3 m^3 concrete pond, which had been thoroughly cleaned and disinfected. They remained in this pond until day 4 post-hatching (DPH), after which they were moved to a 3.5 m^3 circular pond lined with geomembrane. This pond was fertilized two days prior to the larvae transfer with commercial chemical fertilizer (10-30-10, N-P-K) at a rate of 9.6 g/m^2. After hatching, 15 individuals per sample (n = 15) were collected at the time intervals specified in Table 1. The samples were then observed under an optical microscope for a general description, focusing on the most relevant changes in the eyes, mouth, yolk sac, barbels, pigmentation, and other features. The larvae were subsequently measured and euthanized using an overdose of anesthesia through immersion in a clove oil solution (20 mg/L) for fixation. The larval

Table 1
Collection interval of samples of larvae and embryos of capaz (*P. grosskopfii*).

Stage	Interval
Fertilization – hatching	Early stage:10 min Late stage: 30 min
Hatching - three days post-hatching (DPH)	3 hours
4-28 days post-hatching (DPH)	24 hours

development stages were classified according to Nakatani (2001), and Faustino et al., (2010).

All samples were fixed in a 10 % buffered formalin and stored at room temperature. The specimens were processed following standard histological protocols and analyzed using hematoxylin and eosin (H&E) staining and scanning electron microscopy (SEM). These complementary techniques provided detailed visualization of organ development in various body systems, enabling the documentation of critical developmental events and structural transformations throughout ontogeny (Fischer et al., 2008; Martín & Aguado, 2012).

Zootechnical parameters/Morphometric relationships: For the morphometric characterization of *P. grosskopfii* juveniles, 15 individuals (n = 15) were used. The length was measured with an ichthyometer, rounded to the nearest millimeter, and the weight was recorded using a precision digital balance (BBG, JS-1100). Total weight (g) and total length (mm) were recorded. Based on these measurements, the daily weight gain (WG), length gain (LG), and specific growth rate (SGR) were estimated using the following equations:

$$WG = Fw - Iw$$

$$LG = Fl - Il$$

$$SGR = \frac{(Log\ Fw - Log\ Iw)}{t}\ x100$$

Where t is the cultivation time expressed in days, and Ln is the natural logarithm.

Statistical analysis: The experiment used a longitudinal research design to observe the embryonic and larval development of *P. grosskopfii* under controlled conditions. All morphological and zootechnical parameters were analyzed using descriptive statistics and presented as mean ± SD (standard deviation) (Moreno et al., 2019).

RESULTS

In this study, the morphological characteristics during the embryonic development of *P. grosskopfii* larvae under captive conditions were determined and divided into two periods. The embryonic period (up to hatching) includes the stages of zygote, cleavage, blastula, gastrula, segmentation, organogenesis, and hatching. The larval period extended from 0 hours HPH to 15 days DPH. The sequences of morphological changes observed in embryos are presented in Fig. 2, while the sequences of morphological changes and organ development in larvae and juveniles are illustrated in (Fig. 4, Fig. 5, Fig. 6, Fig. 7, Fig. 8, Fig. 9, Fig. 10, Fig. 11, Fig. 12, Fig. 13).

Oocyte morphology and incubation: Freshly spawned *in vivo* oocytes, with a diameter of 1 256 ± 24 µm, are opaque and slightly yellowish. As the fertilized eggs of *P. grosskopfii* hydrate, the cytoplasmic nucleus separates from the innermost layer of the chorion, forming a narrow perivitelline space (Fig. 1). Viable oocytes become translucent, spherical, and pelagic, reaching a maximum diameter of 2 526 µm. They are classified as telolecithal and possess a double chorionic layer, consisting of a thin, smooth, well-defined inner envelope and a second, external gelatinous layer with curved edges. The oocytes are non-adhesive.

The oocytes were incubated at a temperature of 28.0 ± 4.0 °C. The fertilization rate for the batch used in this study was 93.3 ± 1.5 %. During the initial hours, the first cell divisions were synchronized. However, as the number

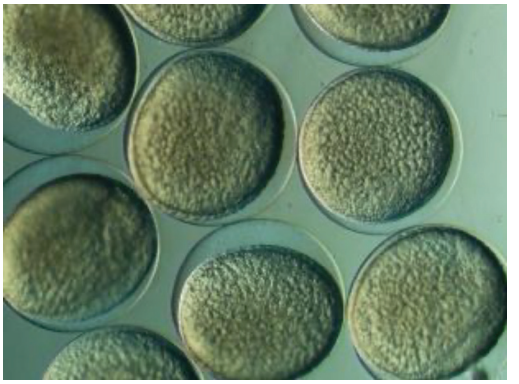

Fig. 1. Newly fertilized oocytes of *P. grosskopfii*, showing little perivitelline space at the beginning of egg hydration.

of blastomeres increased, developmental asynchrony in the embryo occurred.

Embryonic period: Cell divisions following oocyte fertilization in *P. grosskopfii* follow the typical pattern seen in fish eggs.

The duration and characteristics of the different stages of embryonic development are shown in Table 2, and the illustrations during this period can be seen in Fig. 2.

Early larval development: The larval period extended from 0 hours HPH to 15 days DPH. The first stage, the vitelline larva, spans from hatching until the onset of exogenous feeding (mouth and anus opening), followed by the preflexion stage, which begins with exogenous feeding and continues until the initiation of flexion in the terminal region of the notochord (Fig. 3). During this period, the animal undergoes the development of sensory systems (nervous system, sensory receptors related to feeding), osteomuscular systems (bones, muscles, and fins), and digestive systems (gastrointestinal tract organs). The latter is marked by the transition through the different feeding stages (endogenous, endo-exogenous, and exogenous).

Hatching stage: At 11.13 hours post-fertilization (HPF), with a total length (TL) of 4.6 ± 0.5 mm, the cephalic region is attached to the

Table 2

Embryonic development of *P. grosskopfii* at 28 ± 4°C. Percentages in the stages (30, 50, 80, 90 and 95 %) refer to epiboly progression (the physical coverage of the yolk by the blastoderm) and not to statistical variance or time intervals.

Stage	Time post-fertilization (HPF)	Characteristics
Fertilization	0	Fig. 1
Zygote	0.38	Cytoplasm migration and animal pole formation (Fig. 2)
Cleavage (cleaving)	0.47	80 % with 2 cells (blastomeres)
	0.55	80 % with 4 cells (blastomeres)
	0.63	80 % with 8 cells (blastomeres)
	0.72	80 % with 16 cells
	0.88	80 % with 32 cells
	1.05	80 % with 64 cells
Blastula	1.22	80 % with 128 cells
	1.38	80 % with 256 cells
	1.55	80 % with 512 cells
	1.72	1k
	1.97	+ 1k
	2.22	Blastoderm with oblong and sphere
	2.47	dome-30 %
Gastrula	2.72	50 %-germinal ring
	3.13	Embryonic ring and shield
	3.63	Ring -75 % epiboly
	4.63	95 % epiboly - vitelline plug.
Segmentation and organogenesis	5.63	Differentiation of the cephalic and caudal regions and the first three somites appear
	6.13	Optic vesicle and Kupffer's vesicle with six to eight somites
	7.13	Otic vesicle with 12-16 somites
	8.6	20-25 somites, first movements
	9.6	< 25 somites, fast movements
	8.6	Increased head density, heartbeat and blood flow
Hatching	11.6	90 % hatched

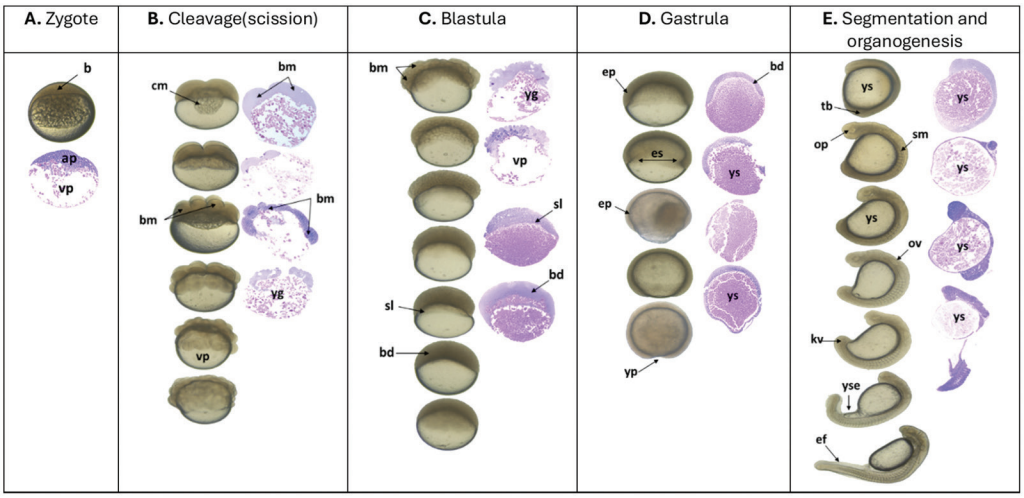

Fig. 2. Description of the embryonic development stages of *P. grosskopfii*. **A.** Zygote stage: One cell with a strongly basophilic-staining area representing the animal pole, and a larger region with eosinophilic granules. **B.** Cleavage stage: from two to 64 cells, during which the first meroblastic divisions occur at the animal pole, dividing in pairs and easily counted. Additionally, the vitelline syncytial layer forms. **C.** Blastula stage: from 128 cells to 30 % epiboly, with a decrease in blastomere size and an enveloping layer that obstructs clear observation of the syncytial layer. **D.** Gastrula stage: from 50 % epiboly to the yolk plug, showing how the enveloping layer covers the entire yolk until the blastopore is closed. **E.** Segmentation and organogenesis stage: from the tail bud to the appearance of somites, which multiply in pairs (from 6 to > 25 somites), with the heart rudiment beating, the first movements, and the appearance of the first sensory organ precursors. Abbreviations: ap: animal pole, b: blastodisc, bd: blastoderm, bm: blastomere, cm: cytoplasmic migration, es: embryonic shield, ef: embryonic fin, ep: epiboly, kv: Kupffer's vesicle, op:optic primordium, ov: otic vesicle, sm: somites, sl: syncytial layer, tb: tail bud, vp: vegetal pole , yg: yolk granules, yp: yolk plug, , ys: yolk sac, yse: yolk sac extension.

anterior part of the yolk sac. A prominent area and a depressed region are visible towards the most rostral part of the head, forming the optic vesicle, with no mouth opening observed (Fig. 3A). In the mid-region, the larva consists of abundant yolk sac (YS), with dark oval-shaped pigmentation in the anterior and caudal areas of the sac. In the caudal region, a tail emerges, with paired cuboid structures separated by a median duct that runs along the length of the larva, extending to the terminal portion. These structures correspond to the myomeres and notochord (egg-shaped clear cells), which will give rise to the muscle mass and spinal cord, respectively. Additionally, a tubular structure is visible extending over the dorsal side of the YS, corresponding to the first traces of the digestive tube (Fig. 3A). This marks the end of the endogenous feeding phase, during which the larvae lack fully developed fins. Instead, there is a membrane that covers and borders the body of the larva. This structure, known as the embryonic fin, enables the larva to perform its first vertical movements.

Histologically, a large yolk sac is observed, containing abundant eosinophilic yolk granules, some of which appear branched (Fig. 4A and Fig. 4B). The yolk sac is surrounded by a thin wall composed of syncytial cells. The cephalic region is notable, primarily consisting of the brain with its divisions (prosencephalon, mesencephalon, and rhombencephalon). Most of the tissue is composed of basophilic cells, indicating the division of histological layers. In the most rostral part of the head, the optic vesicles are visible, though no histological layer differentiation is apparent at this stage. Caudal to the yolk sac, the tail is primarily formed by myomeres separated by myosepta, distributed on both sides of the notochord, which appears

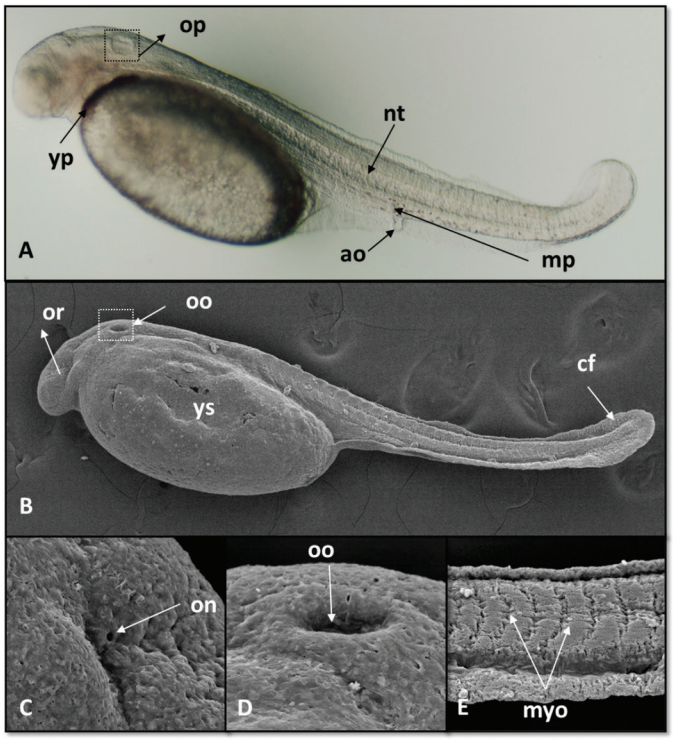

Fig. 3. Anatomical structures present in freshly hatched larvae of *P. grosskopfii*, observed using two techniques (optical microscopy and scanning electron microscopy-SEM). **A.** In vivo larva under optical microscopy (4X), showing the embryonic fin without pigmentation, and the presence of a large yolk sac, as well as rudimentary primordia. **B.** SEM image of the microarchitecture of a newly hatched larva (SEM, 100X). **C.** Cranial region, showing detailed optic rudiment with the presence of the optic nerve (SEM, 2 000X). **D.** Detail of the caudal part of the cephalic region, showing a rudimentary opening (SEM, 2 000X); **E.** Detail of myomeres in the caudal region (SEM, 1 500X). Abbreviations: ao: anal opening, cf: caudal fin, mp: melanophores, myo: myomeres, on: optic nerve, nt: notochord,; oo: opercular opening, op: operculum primordium, or: optic rudiment, yp: yolk pigmentation, ys: yolk sac.

as a cluster of large, round adipose cells with clear cytoplasm and a marginal nucleus.

Upon SEM examination, a depression was observed in the cephalic region, with a tiny foramen at its center (Fig. 4D). The otic vesicle appeared protruding but showed no differentiation of its components or histological layers. In the caudal region of the head, a crateriform structure was noted, which may correspond to the otic vesicle (Fig. 3D). Prominent structures, likely precursors of the operculum and branchial cavity, were also observed (Fig. 3B). Additionally, the myomeres were slightly thickened (Fig. 3E).

Larvae at 1-hour HPH: The optic rudiment is more prominent and exhibits slight pigmentation than the hatching stage. The digestive tube is initially straight, curving towards the posterior region where the rectum and anus will form (Fig. 4A). Point-like pigments (chromatophores) form two rows at the basal part of the ventral myomeres, extending towards the caudal region of the larva. A dark,

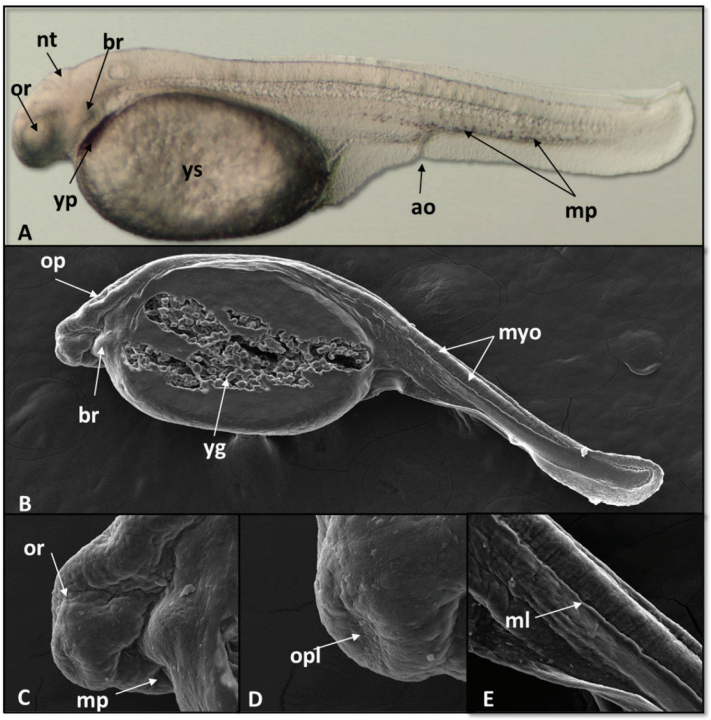

Fig. 4. Anatomical structures present in 1 hour post-hatching (HPH) larvae of *P. grosskopfii* observed using two microscopy techniques (optical microscopy and scanning electron microscopy-SEM). **A.** In vivo larva observed under optical microscopy (4X), showing the embryonic fin, the first pigmented areas, and the presence of the yolk sac, along with more defined rudimentary primordia. **B.** Larval microarchitecture revealing thickening of structures in the cephalic region and exposed yolk granules (SEM, 130X). **C.** Cranial region showing early formations of the mouth and barbels in detail (SEM, 969X). **D.** Detailed view of the choana located in the rostral part of the cephalic region, revealing sensory cells (SEM, 2 000X). **E.** Detailed view of the myomeres in the caudal region, highlighting the definition of the median line (SEM, 1 500X). Abbreviations: mp: mouth primordium, yg: yolk granules, ml: median line, mp: melanophores, myo: myomeres, ao: anal orifice, op: operculum primordium, yp: yolk pigmentation, br: barbel rudiment, or: optic rudiment, ys: yolk sac, nt: neural tube, opl: olfactory placode.

oval-shaped area of pigmentation is prominent between the head and the yolk sac. Perpendicular myomeres, separated by myosepta, are also observed (Fig. 4A).

In SEM, the characteristic features of Siluriformes begin to emerge, including folds (wrinkles) in the skin on the dorsal part of the head. A convex region corresponding to the olfactory placode is also observed (Fig. 4D). Fin differentiation has not yet occurred; however, a faint division line near the yolk sac is evident, along with its granular content (Fig. 4B) and the separation of myomeres by a median line identified as myosepta (Fig. 4E).

Histologically, anterior to the yolk sac, the cephalic region is prominent, with the encephalon and its subdivisions becoming more distinguishable. Two rounded protrusions with bilateral distribution are more cranially observed, corresponding to vesicles that have not yet developed distinct histological layers. Caudal to the yolk sac, a basophilic tubular structure is present in a ventral position, representing the initial remnants of the intestinal tract, though without a clearly defined lumen (Fig. 5B). A small remnant of the caudal fin is also observed at this stage.

In the present study, from 4 hours HPH onwards, a more developed cephalic region is observed, with distinct divisions of the prosencephalon, mesencephalon, and rhombencephalon—structures that occupy a significant

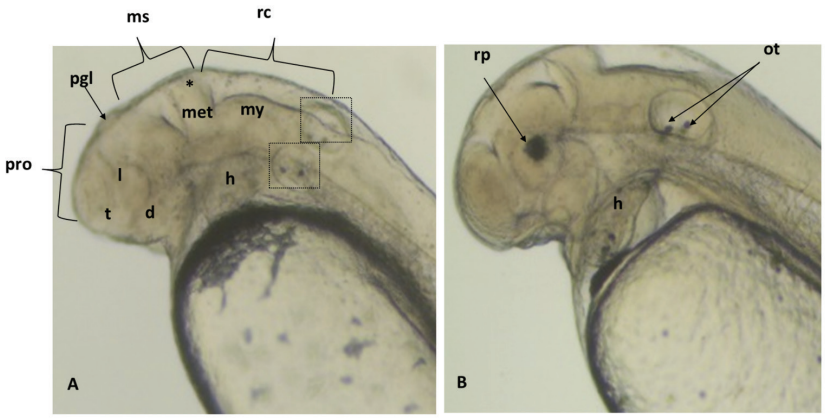

Fig. 5. Comparison of cephalic region development in *P. grosskopfii* Larvae During the First hours post-hatching (HPH) using optical microscopy (10X). **A.** Newly hatched larva showing the central nervous system (CNS) with its three main vesicles: the prosencephalon, divided into the telencephalon and diencephalon, the mesencephalon, and the rhombencephalon. **B.** Larva at 4 hours HPH. Abbreviations: h: heart, l: lens, d: diencephalon, pgl: pineal gland, ms: mesencephalon, met: metencephalon, my: myelencephalon, ot: otoliths, pro: prosencephalon, rp: retinal pigmentation, rc: rhombencephalon, t: telencephalon, (square): otic vesicle, *: future cerebellum.

portion of the head—. This suggests that during these early days, the larvae primarily rely on vision and taste to explore their habitat (Fig. 5B).

Larvae at 13 HPH: The head displayed increased length and morphology typical of a siluriform. A small, narrow oral opening was observed, with the mouth located ventrally. Retinal pigmentation was evident, and chromatophores were visible on the body surface, distributed multifocally in a single row along the ventral region, with some of them present on the dorsal side of the myomeres. Additionally, two strongly pigmented, point-like areas were identified—one in the cranial region of the yolk sac and the other in the caudal region (Fig. 6A). Two short barbels were observed for the first time (Fig. 6).

The yolk sac (YS) showed a significant size reduction, containing yolk granules, some of which appeared branched and were surrounded by a thin wall primarily composed of syncytial cells. The body exhibited more robust myomeres, separated by myosepta, and arranged at a slight incline, forming a V-shape. The ventral fin was observed under optical microscopy and confirmed with SEM, showing a discontinuity with an opening at the midpoint of the fin corresponding to the anal orifice (Fig. 7C). The first indications of the pectoral fin were also visible (Fig. 6D). At this stage, the caudal fin no longer appeared convex, as in earlier stages, but instead adopted a more triangular shape.

Using SEM, two concavities were observed in the rostral region, corresponding to the olfactory area where the nostrils will begin to form. Rounded edges and button-like structures, representing ciliary bundles, were also noted (Fig. 6). In this stage, two crateriform structures were observed in the dorsolateral region of the skull, exhibiting symmetrical bilateral distribution. Additionally, two ventral notches near these openings indicated the operculum formation.

Larvae at 17.5 HPH: The division between the diencephalon, telencephalon, and mesencephalon is observed in the cranial region, with distinguishable histological layers in the brain, including a clear separation between gray and white matter. The eye also shows significant development, with the differentiation of retinal layers, including ganglion cells and pigmentary tissue. Early signs of hyaline cartilage are visible in the skull, marking the onset of chondrocranium formation. The nasomaxillary and opercular regions are defined, although they are not yet fully developed. At the cellular

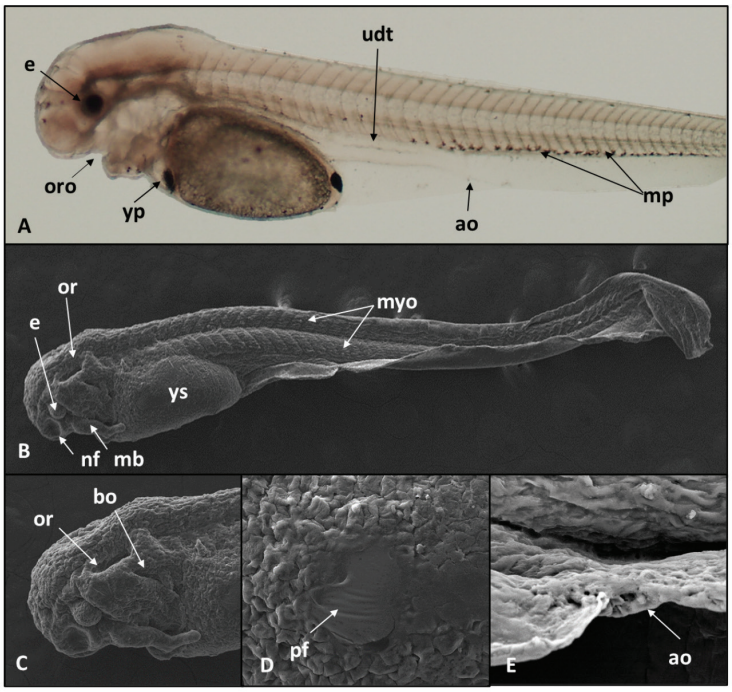

Fig. 6. Anatomical structures present in 13- hours post-hatching (HPH)larvae of *P. grosskopfii*, observed using two techniques: optical microscopy and scanning electron microscopy-SEM). **A.** In vivo larva observed under an optical stereomicroscope (10x), showing the definition of the embryonic fin, increased coverage of pigmented areas, a smaller yolk sac, and a greater myomere density. **B.** Larval microarchitecture, with defined structures in the cephalic region, including the eye, olfactory bulb, and barbels, as well as thickening of the myomeres and increased density and number, confirmed by SEM (70X). **C.** The cranial region shows the definition of the ocular globe, details of the opercular rudiment, and elongation of the barbels (SEM, 400X). **D.** Lateral medial region of the yolk sac, where the radii of the lateral fin primordium are observed (SEM, 1 500X). **E**. Anal region showing the opening of the anal orifice (SEM, Mag 500X. **F.** Caudal region showing the appearance of neuromasts along the midline (SEM, 900X). Abbreviations: ao: anal orifice, bo: branchial opening, e: eye, mb: maxillary barbels, mp: melanophores, myo: myomeres, nf: nasal fossa, nm: neuromasts, pf: pectoral fin, or: opercular rudiment, oro: oral opening, udt: undifferentiated digestive tube, yp: yolk pigmentation, ys: yolk sac.

level, digitiform projections are observed on the lateral side of the head, consistent with branchial filaments. In addition to the two barbels mentioned in earlier stages, short, thin barbels are now visible, projecting from the lateral side of the mouth toward the caudal end. The larva also shows increased length in the caudal region, with myomeres forming a distinct V-shape, separated by myosepta. Furthermore, the ventral and caudal fins enhance development and definition (Fig. 7).

The larva exhibits an elongated mouth, slightly positioned rostrally, with a fully developed oral opening and its first dental structures (~ 4). The onset of the endoexogenous feeding stage is characterized by the detection, capture, and consumption of live prey, with yolk reserves (YR) at approximately 20 %.

Larvae at 31 HPH: The nostrils are fully developed, and the long barbels at this stage feature multiple structures resembling gustatory or sensory corpuscles. Two rows of teeth, ranging from 10 to 14 dental pieces, are visible in the oral cavity. The mouth is fully positioned at the rostral end, and the opercula are completely formed. Unlike in previous stages, a mucocutaneous fold shaped like a rosette is observed on the anus. The caudal fin is triangular, with the first rays clearly visible. By 31 hours of HPH, the yolk sac is fully absorbed, marking the beginning of exogenous feeding (Fig. 8).

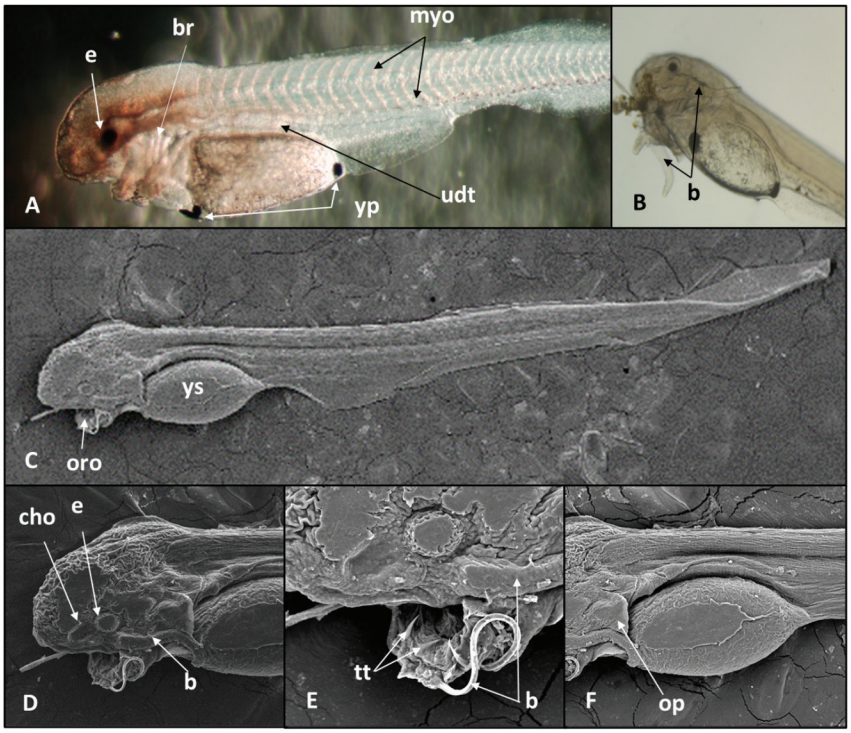

Fig. 7. Anatomical structures present in 17 hours post-hatching (HPH) larvae of *P. grosskopfii*, observed using two microscopy techniques (optical microscopy and scanning electron microscopy-SEM). **A.** In vivo larva observed under an optical stereomicroscope (4X), showing the definition of branchial arches, a reduced yolk sac, and the opening of the gastrointestinal tract mucosa. **B.** In vivo larva observed under an optical stereomicroscope (4X), displaying the cephalic region with details of elongation and the appearance of sensory corpuscles. The onset of hunting behavior is evident, with prey in the mouth. **C.** The organs in the cephalic region begin to be defined, with the oral opening and mouth positioned terminally (SEM, 60X). **D.** Cranial region showing the definition of the ocular globe, choana, and greater definition of the operculum, along with the elongation and differentiation of two pairs of barbels (anterior maxillary and inferior maxillary) (SEM, 300X). **E.** Nasomaxillary region showing the emergence of four dental structures and confirming the thickness and insertion of the two pairs of barbels (SEM, 700X). **F.** Detail of the opercular region (SEM, 300 X). Abbreviations: ao: anal orifice b: barbels, br: branchial arches, , e: eye, im: intestinal mucosa, myo: myomeres, nt: notochord, op: operculum, ot: otoliths, sc: sensory corpuscle, sk: skull, stc: stomach curvature, tt: teeth, dotted circle: sensory corpuscles enlargement.

Larvae at 9 days DPH: The complete opening of the oral cavity was observed, with the mouth in its final position. The oral cavity is lined with non-keratinized stratified squamous epithelium containing mucus-secreting cells. Between four and six rows of teeth were identified, with approximately 30 to 40 teeth per row in both the upper and lower parts of the mouth (Fig. 9). Multiple structures resembling taste buds were observed on the lips. Cartilage was found in both the upper and lower jaws, which will form the premaxillary, maxillary, and dentary bones. This hyaline cartilage comprises perichondrium, chondroblasts, chondrocytes, isogenous groups, and lacunae (Fig. 10A). Groupings of skeletal striated muscle fibers associated with the head were observed. Externally to the mouth, longer barbels were noted, accompanied by numerous sensory corpuscles. Further toward the caudal-ventral region of the oral cavity, the gills were observed, composed of gill arches (hyaline cartilage), filaments, and lamellae with their respective interlamellar spaces (Fig.10A, Fig. 10B).

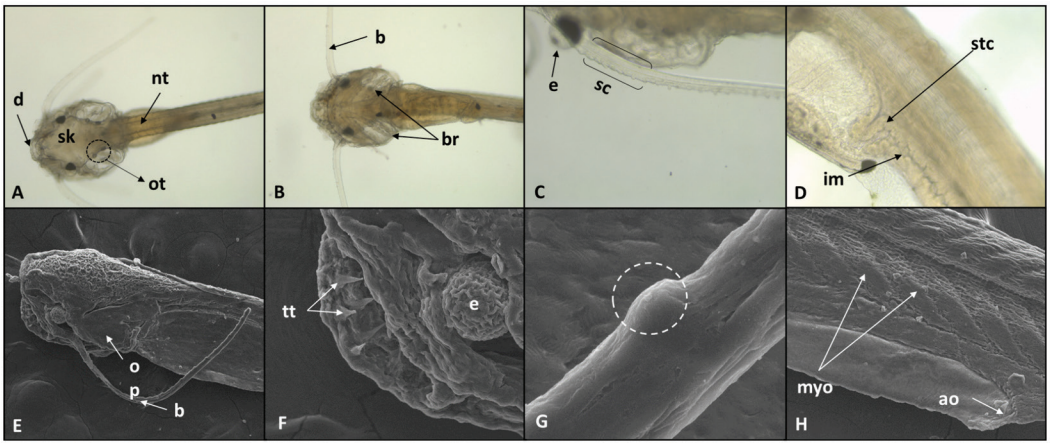

Fig. 8. Anatomical structures present in 31 hours post-hatching (HPH) larvae of *P. grosskopfii*, observed using two microscopy techniques (optical microscopy and scanning electron microscopy-SEM). **A.** In vivo larva observed under an optical stereomicroscope (10X), dorsoventral view, showing chondrocranial structures, otoliths, as well as lips and dental plates. **B.** In vivo larva observed under an optical stereomicroscope (10X), ventrodorsally view, showing four branchial arches and dental plates (anterior maxillary and inferior maxillary), with some dental pieces visible. **C.** In vivo larvae were observed under an optical stereomicroscope (5X), with a magnified view of the ocular globe, separating the lens and retina layers, detailing several sensory corpuscles on the barbels. **D.** In vivo larvae were observed under an optical stereomicroscope (5X) in the abdominal region, showing an "S" shaped curvature of the stomach and the first folds of the intestinal mucosa in the digestive tract. **E.** SEM image showing defined facial structures, the eye within the ocular socket, nasal openings, and elongation of the nostrils and skull, with the mouth open and dental pieces present (SEM, 240X). **F.** Nasomaxillary region shows two rows of teeth, with five dental pieces thicker at the base (SEM, 700X). **G.** Magnified view of the sensory corpuscles on the anterior maxillary barbels (SEM, 5 000x). **H.** Caudal region showing myomeres in a "V" shape (SEM, 600X). Abbreviations: b: barbels, br: branchial arches, c: skull, ce: stomach curvature, cs: sensory corpuscles, d: teeth, mi: intestinal mucosa, mio: myomeres, n: notochord, o: eye, op: operculum, ot: otoliths.

Additionally, the eye in the head displayed a cornea lined with non-keratinized stratified squamous epithelium and the sclera, choroid, and retina. The retina consists of the retinal pigment epithelium, the outer and inner layers of photoreceptors, the external and internal nuclear and plexiform layers, the ganglion cell layer, the nerve fiber layer, and the inner limiting membrane. Furthermore, the brain showed significant development, with observable structures such as the olfactory lobes, optic tectum, cerebellum, medulla oblongata, spinal cord, and ventral to the optic tectum, the hypothalamus.

Histologically, the esophagus was observed posterior to the oral cavity, featuring a mucosal layer lined with stratified cuboidal epithelium containing goblet cells. Beneath this, a layer of loose connective tissue corresponding to the submucosa was present, as no muscularis mucosa was observed. Following this, the muscularis layer consisted of two layers of skeletal striated muscle, with the adventitia located more externally. Further along the gastrointestinal tract, the stomach was found within the coelomic cavity, displaying a mucosal layer composed of simple columnar epithelium, gastric glands, and a layer of loose connective tissue. Beneath this, a submucosa (connective tissue) and, externally, a muscularis layer consisting of two smooth muscle layers, an inner circular and an outer longitudinal layer—were observed. Finally, a thin serosal layer was noted. The anterior, middle, and posterior intestines exhibited a mucosal layer lined with simple columnar epithelium containing goblet cells, a lamina propria composed of loose connective tissue, a muscularis consisting of two layers of smooth muscle, and a thin connective tissue layer corresponding to the serosal tunic. Additionally, multiple digitiform projections

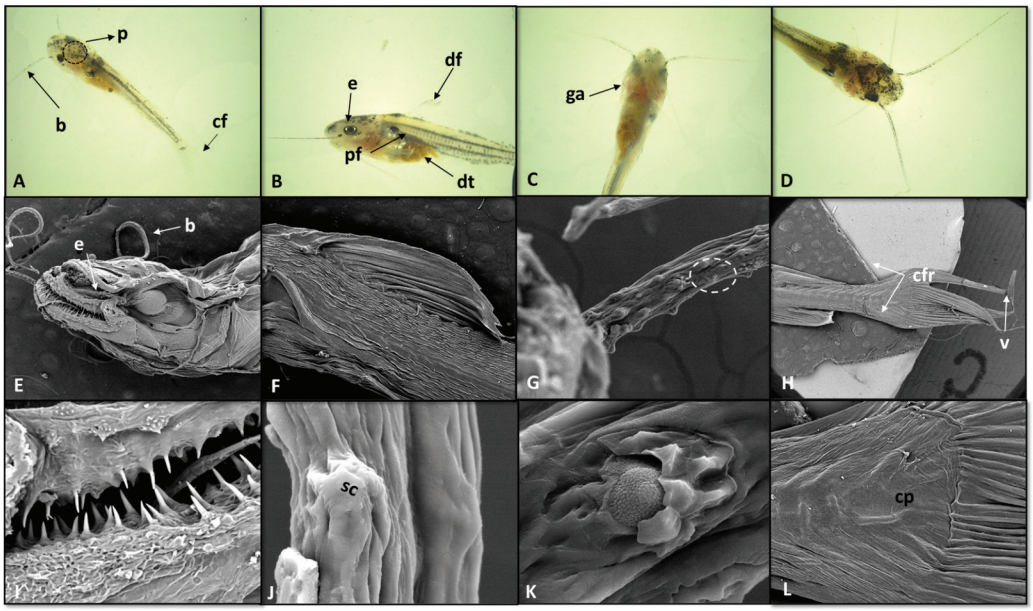

Fig. 9. Anatomical structures present in 9-day old days post-hatching (DPH) *P. grosskopfii* larvae, observed using two microscopy techniques (optical microscopy and scanning electron microscopy-SEM). **A.-D.** Larvae in vivo under an optical stereomicroscope (5X), shown from different angles, with fully developed structures, including a fully developed eye with identifiable components such as the lens, retina, aqueous humor, a defined pigmentation pattern, and a visible abdominal area containing the gastrointestinal tract, heart, and distinct fins with ossified rays. **E.** Cranial region showing capillary structures in the ocular region, as well as the bony structure of the operculum and jaw (SEM, 100X). **F.-H.** Morphology and structure of the rays in the dorsal and caudal fins, respectively, highlighting the hemal and neural spines (SEM, 100X). **G.** Width of the maxillary barbel, showing two types of sensory corpuscles (SEM, 800X). **I.** Nasomaxillary region with two rows of teeth, featuring numerous conical and slender dental pieces, along with sensory corpuscles on the maxillary lips (SEM, 700X). **J.-K.** Sensory structures (circle) and taste buds located on the barbels (SEM, 6 000X). **L.** Magnification of the caudal fin peduncle, revealing vertebrae, neural and hemal spines, and the hypural articulation (SEM, 230X). Abbreviations: cf: caudal fin, df: dorsal fin, pf: pectoral fin, b: barbels, ga: gill arches, sc: sensory corpuscles, e: eye, p: pigmentation, cp: caudal peduncle, cfr: caudal fin rays, dt: digestive tract, v: vertebra.

from the mucosa extended into the lumen. The liver and pancreas were well developed and located adjacent to the stomach. The kidney, positioned at the roof of the coelomic cavity with cranial and caudal portions, and the swim bladder, located in the anterior-dorsal part of the coelomic cavity, were visible at this developmental stage. Both the stomach and intestines contained abundant content, consisting of crustacean remains and organic matter. The osteomuscular system was characterized primarily by a cartilaginous skeleton and numerous myomeres, both epaxial and hypaxial, with a helical morphology and separated by myosepta. The dorsal and caudal fins were visible, each displaying cartilaginous fin rays. Optical microscopy revealed a greater presence of pigments in the body and head (~ 6 rows). The digestive tract showed more advanced development and a brownish coloration, like the gills.

Juvenile at 14 DPH: Histologically, a more advanced stage of development was observed compared to earlier stages. Both the upper and lower jaws displayed the premaxillary, maxillary, and dentary cartilages, composed of hyaline cartilage with their corresponding perichondrium, chondroblasts, chondrocytes, isogenous groups, and lacunae. In the anterior region above the upper jaw, the olfactory

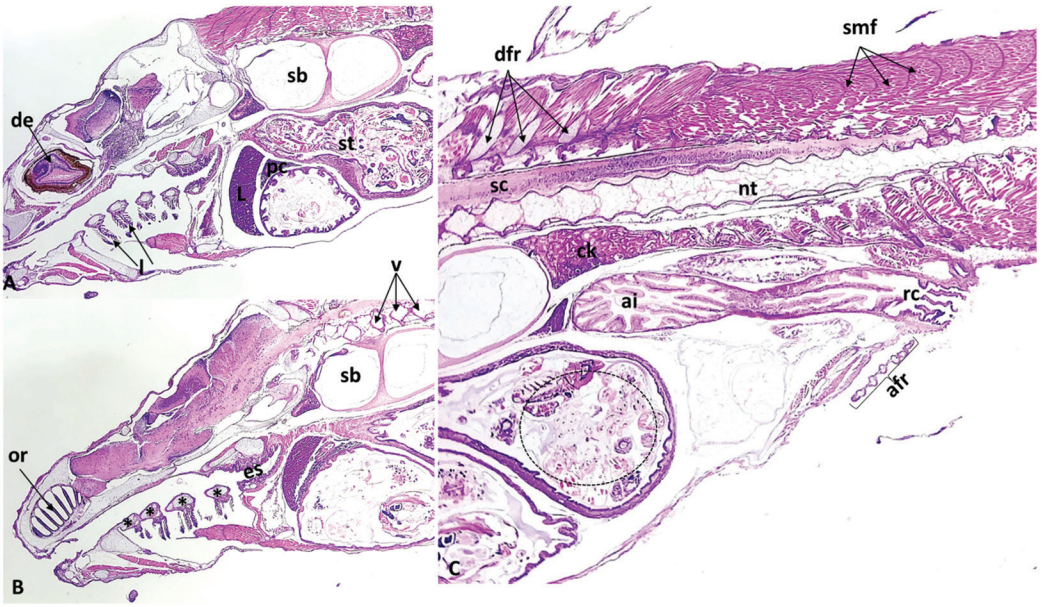

Fig. 10. Longitudinal section of 9-day old days post-hatching (DPH) *P. grosskopfii* larvae. **A.** Superficial view of the cranial region, showing the layers of the retina in the eye, hyaline cartilage of Merckel's bone, the lower jaw, and the upper jaw. **B.** Deep view of the cranial region. **C.** General view of the mid-region, displaying the microstructure of various organs with complete development. Abbreviations: es: esophagus; st: stomach; smf: skeletal muscle fibers; L: liver; ai: anterior intestine; l: lamellae; sc: spinal cord; nt: notochord; de: developed eye; pc: pancreas; afr: anal fin rays; dfr: dorsal fin ray; rc: rectum; ck: cranial kidney; or: olfactory rosette; v: vertebrae; sb: swim bladder; (*) gill arch cartilages; dotted circle: stomach contents.

rosette was identified, with its olfactory epithelium composed of multiple lamellae. The sensory epithelium was supported by a delicate fibrovascular stroma (lamina propria), surrounded by a capsule known as the rosette capsule (Fig. 11). At this stage, four pairs of gill arches were visible on both sides of the head, still made of hyaline cartilage. The filaments were more elongated than in previous stages, as were the lamellae. Striated skeletal muscle at the base of the filaments was also visible, along with the lamellae and their respective interlamellar spaces.

Additionally, both the exocrine and endocrine portions of the pancreas were visible. The kidney, located on the roof of the coelomic cavity with its cranial and caudal portions, as well as the swim bladder in the anterior-dorsal part of the coelomic cavity, were also visible at this developmental stage. Both the stomach and intestines contained abundant content, which appeared to be remains of crustaceans and organic matter (Fig. 12). The osteomuscular system was primarily characterized by a cartilaginous skeleton and abundant myomeres, both epaxial and hypaxial, with a helical morphology separated by myosepta. The dorsal and caudal fins were visible, both exhibiting cartilaginous rays. At this stage, some cartilages began the process of ossification, mainly in the spine.

Zootechnical parameters: At the end of the larviculture period (28 days) (Fig. 13), the weight gain (G) was 0.38 g, with an average increase of 0.014 g/day. The length gain (Gl) was 18 mm, and the growth rate (G) was 19.9 %/day.

Slow growth is observed in the chart during the first six days. After the seventh day, a slight increase occurs, but growth stagnates until day 11 DPH. This stagnation is believed to be a result of the larvae being transferred to 3 m diameter tanks with inoculated zooplankton

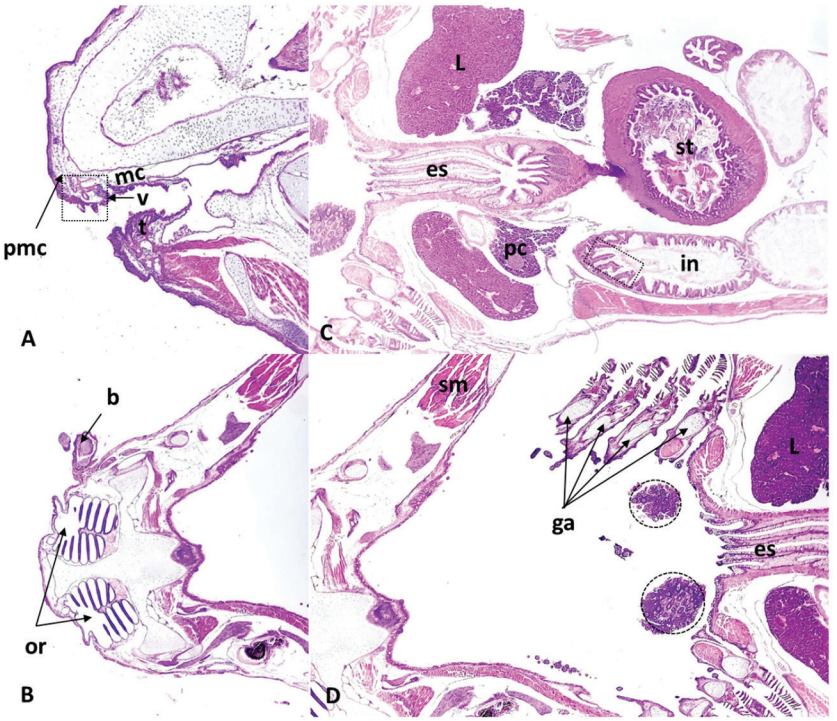

Fig. 11. Longitudinal section of the cranial and mid-regions of 14-day-old days post-hatching (DPH) *P. grosskopfii* larvae (H&E). **A.** Anterior view of the nasomaxillary region, showing cartilaginous cells in the maxillary bones and dental structures. **B.** Cross-section of the premaxillary bone, highlighting the lamellae of the olfactory rosettes. **C.** Longitudinal section of the abdominal region, revealing the cellular structure of the esophagus, stomach, intestine with intestinal folds, and the liver and pancreas. **D.** Cross-section of the lower maxillary region, displaying parts of the gill arches with cartilage and gill filaments, as well as portions of the esophagus and liver. Abbreviations: ga: gill arches; b: barbels; mc: maxillary cartilage; pmc: premaxillary cartilage; vt: villiform teeth (square); es: esophagus; st: stomach; L: liver; in: intestine; pc: pancreas; ro: olfactory rosette; sm: skeletal muscle; (dashed rectangle): intestinal folds; (circle): cartilage.

starting at 5 DPH. Additionally, this stagnation is thought to be caused by the larvae adapting to the new environment. After 12 DPH, growth resumes and continues until the end of the trial, suggesting the potential complete development of the digestive and other sensory organs.

DISCUSSION

The embryonic development of *P. grosskopfii* followed a sequence of morphological stages (zygote, cleavage, blastula, gastrula, segmentation, organogenesis, pharyngula, and hatching) that aligns with the pattern described for other teleost species, including *D. rerio* (Kimmel et al., 1995) and *C. trutta* (Zadmajid et al., 2017).

Regarding oocyte morphology, their classification as telolecithal, as in most teleosts, is due to the yolk being evenly distributed and located only at the animal pole of the cytoplasm, with a large concentration of yolk at the vegetal pole (Da Rocha Perini et al., 2010). The yellowish coloration of the oocytes is characteristic of Siluriformes (Marques et al., 2008; Sato, 1999) and is associated with the presence of carotenoid pigments derived from the food supplied to the breeders. These pigments serve as a source of endogenous oxygen in the event of inefficiency in obtaining exogenous oxygen (Da Rocha Perini et al., 2010; De Amorim et al., 2009).

According to Gomes et al. (2007), the gelatinous envelope and double chorion are

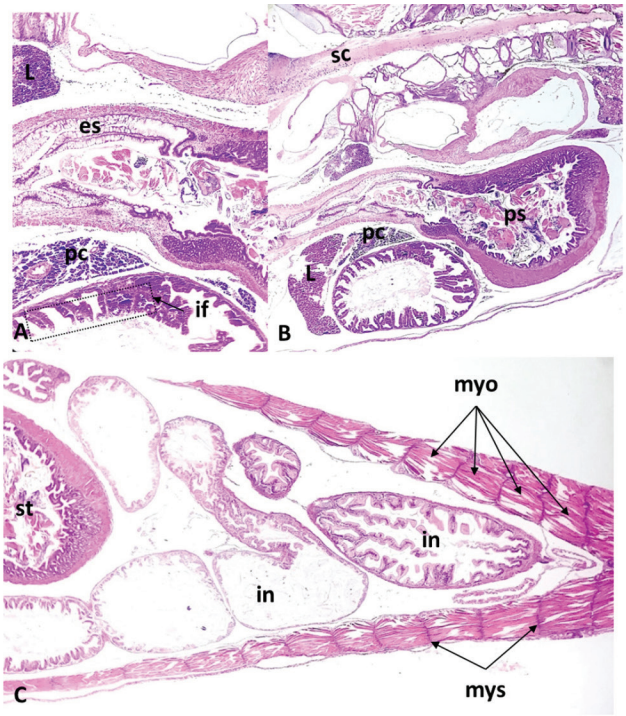

Fig. 12. Longitudinal section of the cranial and mid-regions of 14- days post-hatching (DPH) *P. grosskopfii* juveniles (H&E). **A.** Sagittal section of the abdominal region, showing the stomach and organs with microstructure, including the liver, pancreas, and accessory glands. **B.** Sagittal section of the mid-abdominal region, revealing the microstructure of the organs, including the pyloric stomach. **C.** Transverse section of the caudal abdominal region, showing segments of the intestine, with visible intestinal folds, skeletal muscle fibers (myomeres), and lamellae (myosepta). Abbreviations: es: esophagus; st: stomach; ps: pyloric stomach; L: liver; in: intestine; sc: spinal cord; myo: myomeres; mys: myosepta; if: intestinal folds (dashed rectangle); pc: pancreas; v: vertebra.

found in most Siluriformes and can be either adhesive or non-adhesive. This is like what has been observed in other related species, such as *Pseudoplatystoma coruscans* (Landines et al., 2003), *Rhinelepis aspera* (Da Rocha Perini et al., 2010), and surubí hybrids such as *Pseudoplatystoma coruscans* x *Pseudoplatystoma fasciatum* (Faustino et al., 2007). Further research is needed to better understand the composition, function, and relationship between the gelatinous layer and its adhesion.

On the other hand, during maximum hydration of the oocytes, the diameter increased (diameter = 2 526 µm) in *P. grosskopfii*, which was larger than the values obtained for *Pimelodus maculatus* (Luz et al., 2001) 812 µm for non-hydrated eggs and 1 066 µm for hydrated eggs. However, it was like those of other species of *Pimelodus* reported by Sato (1999): 1 200 µm (non-hydrated) and 1 950 µm (hydrated eggs). Additionally, a perivitelline space was observed, similar to other Siluriformes species such as *Sorubim cuspicaudus* (diameter = 3 579.0 ± 4 97.8 µm) (Novoa & Cataño-Vergara, 2005) and *Pimelodus yuma* (diameter = 1 495.4 ± 33 µm) (Buzollo et al., 2011) as well as Characiformes such as *P. magdalenae*, which possesses eggs with a large perivitelline space (Yepes-Blandón et al., 2022). It is suggested that the wide perivitelline space functions as a protective sac for the embryo, preventing injuries caused by environmental stresses and promoting progeny survival. In *P. maculatus* eggs, following hydration, a reduced perivitelline space is

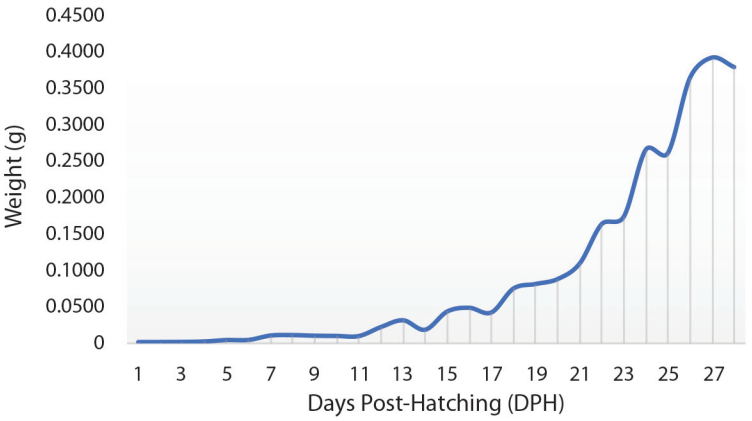

Fig. 13. Growth curve of the capaz (*P. grosskopfii*) for 28 days post-hatching (DPH).

observed (Buzollo et al., 2011), which contrasts with the results obtained in this study. This size difference between teleosts is believed to arise from the different reproductive strategies among the species mentioned and the environments in which their eggs develop (Gomila & Luján, 2015).

The embryonic development of *P. grosskopfii* observed in this study was consistent with previous reports for the species (Valbuena-Villarreal et al., 2012). However, for the first time, we describe the presence of pigmentation in the larva before hatching, which becomes more pronounced during the first hours of larval development. Oliveira-Almeida et al. (2015) also reported the coloration of the yolk sac, both before and after hatching, in another species of Pimelodidae, i.e., *Leiarius marmoratus*.

The vitelline syncytial layer (VSL) is a group of blastomeres (deep cells) that remain attached to the yolk. It begins to form during the early stages of epiboly as the blastomeres divide (Bruce, 2016; Kondakova & Efremov, 2014). This layer is considered an extra-embryonic organ specific to teleosts and plays critical roles throughout embryonic development. It provides microenvironments for molecular feedback, cellular interactions, and mechanical signaling, facilitating morphogenetic movements in the early embryo and during organogenesis (Concha & Reig, 2022; Kimmel et al., 1995). According to the findings of Cardoso et al. (1995) in the embryogenesis of *P. coruscans*, and the formation of this layer during the blastula stage in our study parallels the observations of González-Doncel et al. (2008) in *Oryzias latipes*.

In the present study, the gastrula stage ends with the complete closure of the yolk plug, consistent with previous reports in other Pimelodidae species (Buzollo et al., 2011; Honji et al., 2012) and in Characidae (Botta et al., 2010; Zadmajid et al., 2017). However, Morrison et al. (2001) found that in species such as *Oreochromis niloticus*, the yolk cell is large, preventing the blastoderm from extending across the entire vegetal pole. As a result, rudimentary organogenesis (somite segmentation) begins before the completion of epiboly and the formation of the yolk plug.

The duration of embryonic development in *P. grosskopfii* is like that reported for other specimens of the Pimelodidae family, including *P. coruscans* (Landines et al., 2003; Marques et al., 2008), *P. yuma* (11 HPF at 29.9 ± 0.5 °C) (Oliveira-Almeida et al., 2015), and *P. maculatus* (Buzollo et al., 2011). However, the development rate in *P. grosskopfii* is faster than that observed for *Zungaro jahu* (13 HPF at 29.4 ± 1.5 °C) (Marques et al., 2017) and *S. cuspicaudus* (14.3 ± 0.58 HPF at 28.1 ± 0.5 °C) (Novoa & Cataño-Vergara, 2005). Temporal variations

in ontogeny, feeding physiology, and behavior should be considered, even within the same family (Rønnestad et al., 2013; Valbuena-Villarreal et al., 2012). Furthermore, these variations depend not only on the species or individual but also on environmental conditions. Temperature has been shown to directly affect physiological and metabolic processes, leading to asynchrony during different stages of embryonic development (Kimmel et al., 1995; Lencer & McCune, 2018).

In the present study, the larvae exhibited a faster hatching rate and a higher mean total length than the values reported by Valbuena-Villarreal et al. (2012) for the same species. In *P. yuma*, hatching was reported at 11 HPF (29.9 ± 0.5 °C) with larvae measuring 2.11 ± 0.3 mm in total length (Oliveira-Almeida et al., 2015), while in *S. cuspicaudus*, hatching occurred at 14.3 ± 0.58 HPF (28.1 ± 0.5 °C) with larvae measuring 3.32 ± 0.010 mm in total length (Novoa & Cataño-Vergara, 2005).

In the present study, from 4 HPF onwards, the anterior region of the neural tube expanded into layers, giving rise to the prosencephalon, mesencephalon, and rhombencephalon. This pattern is consistent with previous descriptions in *Rhamdia quelen* (Cussac & Maggese, 1987), *P. coruscans* (Marques et al., 2008), *Prochilodus lineatus* (Ninhaus-Silveira et al., 2006), *L. marmoratus* (Oliveira-Almeida et al., 2015), and *D. rerio* (Espiñeira Cotos, 2017). The rapid development of these structures suggests that individuals must quickly perceive their environment, adapt, and survive in their natural habitat (Londoño & Hurtado Giraldo, 2010).

The yolk sac coloration of *P. grosskopfii* postlarvae is similar to that reported for *Pseudoplatystoma fasciatum* (Andrade et al., 2016) and *P. maculatus* (Buzollo et al., 2011). This pigmentation may help larvae camouflage within their natural environment during the first days of life (Kossowski & Madrid, 1991).

In the present study, pigmentation intensified and was irregularly distributed. Chromatophores began migrating throughout the body, using pseudopodia for movement, and subsequently changed from a puncture to a dendritic shape. Some fish species exhibit only dendritic chromatophores, such as *R. aspera* (Da Rocha Perini et al., 2010), while others have only punctate chromatophores, as observed in *R. quelen* (De Amorim et al., 2009), *Hoplias lacerdae,* and *Hoplerythrinus unitaeniatus* (Gomes et al., 2007). In contrast, *Hoplias malabaricus* (Gomes et al., 2007) exhibits both types, like the observations in this study.

Retinal pigmentation does not follow a defined pattern across neotropical fish species and begins at different stages of development. In some species, pigmentation occurs before hatching, as observed in *D. rerio* (Kimmel et al., 1995) and *Hemiramphus brasiliensis* (Rosas et al., 2008). However, species such as *Z. jahu* (Nogueira et al., 2012) and *Hemisorubim platyrhynchos* (Faccioli et al., 2016) display patterns similar to those of *P. grosskopfii*.

In *P. grosskopfii*, barbicel rudiments appear at 13 HPF. These structures have also been described in *P. fasciatum*, where their appearance is reported at 21 HPF (Andrade et al., 2016), in *Pseudoplatystoma reticulatum* at 12 HPF (Andrade et al., 2016) and in *R. quelen* at 10 HPF (Rodrigues-Galdino et al., 2010). Barbicels are important accessory structures for feeding and sensory perception of the environment. The timing of their appearance varies according to species and feeding habits. In general, carnivorous species exhibit faster development of these structures (Al-Nusear et al., 2022; Elliott, 2000).

On the other hand, at 13 HPF, structures resembling buttons, corresponding to ciliary bundles, are observed in the olfactory area (Fig. 9). These structures have also been described in *Pseudoplatystoma corrugans* at 25 HPF (Cestarolli, 2005). The appearance of these structures may suggest that these animals rely on sensory mechanisms (mechanical or chemical) in addition to vision for food detection and interaction with their environment (Hansen & Zielinski, 2005).

In *P. grosskopfii*, yolk reserve consumption increased rapidly during the first hours of larval life, and by 13 HPF, the yolk sac accounted for only 30 % of the larva's body. These results

are typical for teleost larvae, such as *Oplegnathus fasciatus* and *Platax teira* (He et al., 2011; Zeng et al., 2020), among others. Additionally, this coincided with the accelerated growth and development of the digestive tract (mouth opening, anal pore) and locomotor system during the same period. These events occur almost simultaneously, as they are closely linked to the onset of exogenous feeding in fish, which may occur either before the yolk sac is completely depleted or after it is exhausted, depending on the characteristics of each species (Moncaleano et al., 2018; Yúfera & Darias, 2007).

The onset of endoexogenous feeding in *P. grosskopfii* occurred at 17.5 HPF, with approximately 20 % of YR remaining. As observed in other teleosts, exogenous feeding begins before the complete absorption of the yolk sac. However, the timing and percentage of reserves vary, as seen in *L. marmoratus*, where 10 % YR was observed at 35 HPF and less than 10 % at 40 HPF (Ramírez-Merlano et al., 2010). In contrast, in siluriforms like *S. cuspicaudus*, endoexogenous feeding began between 46 and 48 HPF with 52.8 % YR (Valbuena-Villarreal et al., 2012), and in *P. magdalenae,* feeding began between 44 and 48 HPF with 34 % YR (Atencio García et al., 2003). These findings highlight the high voracity of these species at the onset of exogenous feeding, with, in some cases, the initiation of exogenous feeding coinciding with the near-total consumption of the yolk sac (Gisbert & Williot, 2002).

The onset of exogenous feeding and complete reabsorption of the yolk sac occurred at 17.5 HPF in *P. grosskopfii,* which is faster than what has been reported for *H. platyrhynchos*, where the yolk sac persists until 4 DPH (Faccioli et al., 2016), *Silurus glanis* (Kozarić et al., 2008), and *R. quelen* (De Amorim et al., 2009). In contrast, *Ompok bimaculatus* yolk sacs last up to 5 DPH (Pradhan et al., 2013), while in *Piaractus mesopotamicus*, they remain until 4-5 DPH at 26-28 °C, and in *Prochilodus argenteus*, until 4 DPH at 23 °C (Portella et al., 2014).

In *P. grosskopfii*, the liver is situated laterally within the anterodorsal region of the coelomic cavity. Although it is not a distinctly lobulated organ, it can be described as consisting of two hepatic segments (left and right lobes). This anatomical presentation contrasts with observations in other neotropical fish, such as *H. platyrhynchos* (Faccioli et al., 2014), which feature a bilobate liver, and *H. malabaricus* (Lemes & Braccini, 2004), which has three lobes. Histologically, hepatocytes, hepatic sinusoids, bile canaliculi, and intrahepatic exocrine pancreatic tissue are observed in the ventral portions of the liver at all developmental stages. Nevertheless, since the pancreatic tissue and the liver are not fused, the term "intrahepatic pancreas" is a more precise description than "hepatopancreas." This arrangement is different from that of other actinopterygian species, in which the pancreas appears as a compact, oval-shaped body embedded in the mesenteric adipose tissue located between the spleen and intestinal loops (Chanet et al., 2023).

The embryonic period of *P. grosskopfii* lasts 11.6 hours HPF at 28.4 ± 1.1 °C. The newly hatched larva measures a total length of 4.6 ± 0.5 mm. At 13 HPF, the primordia of the barbels are observed, and exogenous feeding begins between 17 and 18 HPF or 30 HPF. The yolk reserves are completely reabsorbed by 31 HPF. By 14 days DPH, ossification of most mandibular elements is complete, including the premaxillary, maxillary, and dentary bones. At 9 DPH, the dorsal, caudal, and anal fins show bony rays, the eyes are fully developed with abundant vascularization, and differentiation of their various structures—such as the cornea, sclera, lens, retina with its complete layers, iris, and choroid—can be observed. By 14 DPH, ossification primarily affects the vertebral column. In general, the embryogenesis and larval development of *P. grosskopfii* followed the typical pattern of teleosts in the order Siluriformes, characterized by rapid larval development. It is evident that the development of *P. grosskopfii* larvae begins with the structures primarily responsible for environmental recognition, sensory organs, and motor coordination. The movement coordination for prey capture becomes crucial because *P. grosskopfii* is zooplanktivorous during these early stages.

Ethical statement: The authors declare that they all agree with this publication and made significant contributions; that there is no conflict of interest of any kind; and that we followed all pertinent ethical and legal procedures and requirements. All financial sources are fully and clearly stated in the acknowledgments section. A signed document has been filed in the journal archives.

ACKNOWLEDGMENTS

The authors thank Piscícola San Silvestre S.A. and HISTOLAB for their technical contribution within the framework of the Management Program for protecting fish and fishing resources of the Sogamoso River and its floodplain. This work was funded by ISAGEN S.A. (agreement 33/121 and 33/02168 ISAGEN-UdeA).

REFERENCES

Albus, U. (2012). Guide for the Care and Use of Laboratory Animals (8th edn). *Laboratory Animals*, *46*(3), 267–268. https://doi.org/10.1258/la.2012.150312

Al-Nusear, A. N., Abed, R. I., & Abdulsamad, S. M. (2022). Histological study of maxillary barbels in Silurus triostegus and Heteropneustes fossilis (Siluriformes) fishes collected from Basra City waters. *Samarra Journal of Pure and Applied Science, 4*(2). https://www.iasj.net/iasj/download/a916c5e86b35ee3f

Andrade, F. F., Lima, A. F., Assumpção, L., Makrakis, S., Kasai, R. I. D., & Makrakis, M. C. (2016). Characterization of the early development of *Pseudoplatystoma reticulatum* Eigenmann & Eigenmann, 1889 (Siluriformes: Pimelodidae) from the Paraguay River Basin. *Neotropical Ichthyology, 14*, e150032. https://doi.org/10.1590/1982-0224-20150032

Arias-Gallo, M., Jiménez-Segura, L. F., & Dorado, M. del P. (2010). Desarrollo larval de *Prochilodus magdalenae* (Steindachner, 1879) (Pisces: Prochilodontidae), río Magdalena, Colombia. *Actualidades Biológicas, 32*(93), 199–208.

Atencio García, V., Kerguelén, E., Wadnipar, L., & Narváez, A. (2003). Manejo de la primera alimentación del bocachico (*Prochilodus magdalenae*). *Revista MVZ Córdoba, 8*(1), 254–260.

Atencio-García, V., & Zaniboni-Filho, E. (2006). El canibalismo en la larvicultura de peces. *Revista MVZ Córdoba*, *11*(Supl), 9–19. https://doi.org/10.21897/rmvz.1040

Atencio, V., Buelvas, V. M. P., Espitia, F. P., Mestra, R. O., & Carrasco, S. C. P. (2010). Manejo de la primera alimentación de dorada (Brycon sinuensis) ofreciendo larvas de bocachico (Prochilodus magdalenae). *Revista Colombiana de Ciencias Pecuarias, 23*(3), 317–324. https://doi.org/10.17533/udea.rccp.324593

Botta, P., Sciara, A., Arranz, S., Murgas, L. D. S., Pereira, G. J. M., & Oberlender, G. (2010). Estudio del desarrollo embrionario del sábalo (*Prochilodus lineatus*). *Archivos de Medicina Veterinaria, 42*(2), 109–114. https://doi.org/10.4067/S0301-732X2010000200014

Bruce, A. E. E. (2016). Zebrafish epiboly: Spreading thin over the yolk. *Developmental Dynamics, 245*(3), 244–258. https://doi.org/10.1002/dvdy.24353

Buzollo, H., Veríssimo-Silveira, R., Oliveira-Almeida, I. R., Alexandre, J. S., Okuda, H. T., & Ninhaus-Silveira, A. (2011). Structural analysis of the *Pimelodus maculatus* (Lacépède, 1803) embryogenesis (Siluriformes: Pimelodidae). *Neotropical Ichthyology, 9*, 601–616. https://doi.org/10.1590/S1679-62252011000300013

Cala Cala, P. (2019). *Medio ambiente y diversidad de los peces de agua dulce de Colombia*. Academia Colombiana de Ciencias Exactas, Físicas y Naturales. https://repositorio.accefyn.org.co/handle/001/2384

Cardoso, E. L., Alves, M. S. D., Ferreira, R. M. A., & Godinho, H. P. (1995). Embryogenesis of the neotropical freshwater Siluriforme *Pseudoplatystoma coruscans*. *Aquatic Living Resources, 8*(4), 343–351. https://doi.org/10.1051/alr:1995037

Castro-Ruiz, D., Mozanzadeh, M. T., Fernández-Méndez, C., Andree, K. B., García-Dávila, C., Cahu, C., Gisbert, E., & Darias, M. J. (2019). Ontogeny of the digestive enzyme activity of the Amazonian pimelodid catfish *Pseudoplatystoma punctifer* (Castelnau, 1855). *Aquaculture, 504*, 210–218. https://doi.org/10.1016/j.aquaculture.2019.01.059

Cestarolli, M. A. (2005). *Larvicultura do pintado Pseudoplatystoma coruscans (Agassiz, 1829): Aspectos da alimentação inicial e do desenvolvimento de estruturas sensoriais* [Tesis de maestría, Universidade Estadual Paulista]. http://hdl.handle.net/11449/144162

Chanet, B., Schnell, N. K., Guintard, C., & Chen, W. J. (2023). Anatomy of the endocrine pancreas in actinopterygian fishes and its phylogenetic implications. *Scientific Reports, 13*(1), 22501. https://doi.org/10.1038/s41598-023-49404-

Collazos-Lasso, L. F., Gutiérrez-Espinosa, M. C., & Restrepo-Betancur, L. F. (2014). Supervivencia de larvas de cachama blanca, *Piaractus brachypomus* Cuvier, 1818, sometidas a cambios experimentales de temperatura. *Orinoquia, 18*, 193–197.

Concha, M. L., & Reig, G. (2022). Origin, form and function of extraembryonic structures in teleost fishes. *Philosophical Transactions of the Royal Society B: Biological Sciences, 377*(1865), 20210264. https://doi.org/10.1098/rstb.2021.0264

Cussac, V., & Maggese, M. C. (1987). Seasonal changes in the presumptive gonadotrophic cells of the catfish *Rhamdia sapo* (Pisces, Pimelodidae) in relation to gonadosomatic index. *Comunicaciones Biológicas, 6*(2), 113–123.

Da Rocha Perini, V., Sato, Y., Rizzo, E., & Bazzoli, N. (2010). Biology of eggs, embryos and larvae of *Rhinelepis aspera* (Spix & Agassiz, 1829) (Pisces: Siluriformes). *Zygote, 18*(2), 159–171. https://doi.org/10.1017/S0967199409990165

De Amorim, M. P., Gomes, B. V. C., Martins, Y. S., Sato, Y., Rizzo, E., & Bazzoli, N. (2009). Early development of the silver catfish *Rhamdia quelen* (Quoy & Gaimard, 1824) (Pisces: Heptapteridae) from the São Francisco River Basin, Brazil. *Aquaculture Research, 40*(2), 210–219. https://doi.org/10.1111/j.1365-2109.2008.02079.x

Díaz-Olarte, J., Marciales-Caro, L. J., Cristancho Vásquez, F., & Cruz-Casallas, P. E. (2010). Comparison of the embryonic development of *Piaractus brachypomus* (Serrasalmidae) and *Pseudoplatystoma* sp. (Pimelodidae). *International Journal of Morphology, 28*(4), 1193–1204. https://doi.org/10.4067/S0717-95022010000400033

Elliott, D. G. (2000). Integumentary system. In G. K. Ostrander (Ed.), *The laboratory fish* (pp. 271–306). Academic Press. https://doi.org/10.1016/B978-012529650-2/50023-8

Espiñeira Cotos, L. (2017). *Estudio experimental de las conexiones neuronales de los núcleos pretectales en el pez cebra (Danio rerio)* [Tesis doctoral, Universidade da Coruña]. https://ruc.udc.es/dspace/handle/2183/19247

Faccioli, C. K., Chedid, R. A., Bombonato, M. T. S., Vicentini, C. A., & Vicentini, I. B. F. (2014). Morfología e histoquímica del hígado del pez carnívoro *Hemisorubim platyrhynchos*. *International Journal of Morphology, 32*(2), 715–720. https://doi.org/10.4067/S0717-95022014000200055

Faccioli, C. K., Chedid, R. A., Mori, R. H., do Amaral, A. C., Belmont, R. A. F., Vicentini, I. B. F., & Vicentini, C. A. (2016). Organogenesis of the digestive system in Neotropical carnivorous freshwater catfish *Hemisorubim platyrhynchos* (Siluriformes: Pimelodidae). *Aquaculture, 451*, 205–212. https://doi.org/10.1016/j.aquaculture.2015.09.009

Faustino, F., Nakaghi, L. S. O., Marques, C., Ganeco, L. N., & Makino, L. C. (2010). Structural and ultrastructural characterization of the embryonic development of *Pseudoplatystoma* spp. hybrids. *The International Journal of Developmental Biology, 54*(4), 723–730. https://doi.org/10.1387/ijdb.082826ff

Faustino, F., Nakaghi, L. S. O., Marques, C., Makino, L. C., & Senhorini, J. A. (2007). Fertilização e desenvolvimento embrionário: Morfometria e análise estereomicroscópica dos ovos dos híbridos de surubins (pintado, *Pseudoplatystoma coruscans* × cachara, *Pseudoplatystoma fasciatum*). *Acta Scientiarum. Biological Sciences, 29*(1), 49–55. https://doi.org/10.4025/actascibiolsci.v29i1.126

Fischer, A. H., Jacobson, K. A., Rose, J., & Zeller, R. (2008). Hematoxylin and eosin staining of tissue and cell sections. *Cold Spring Harbor Protocols, 2008*(5). https://doi.org/10.1101/pdb.prot4986

Gisbert, E., & Williot, P. (2002). Advances in the larval rearing of Siberian sturgeon. *Journal of Fish Biology, 60*(5), 1071–1092. https://doi.org/10.1111/j.1095-8649.2002.tb01705.x

Gomes, B. V. C., Scarpelli, R. S., Arantes, F. P., Sato, Y., Bazzoli, N., & Rizzo, E. (2007). Comparative oocyte morphology and early development in three species of trahiras from the São Francisco River basin, Brazil. *Journal of Fish Biology, 70*(5), 1412–1429. https://doi.org/10.1111/j.1095-8649.2007.01420.x

Gomila, V., & Luján, G. (2015). *Estrategias reproductivas de las especies de peces óseos más conspicuas y abundantes en los arrecifes rocosos costeros de la Patagonia norte* [Tesis doctoral, Universidad de Buenos Aires, Facultad de Ciencias Exactas y Naturales]. https://bibliotecadigital.exactas.uba.ar/collection/tesis/document/tesis_n6058_VillanuevaGomila

González, J., Landines, M. A., Borbón, J., Correal, M. L., Sánchez, C., & Rodríguez, L. (2014). Evaluación de algunos marcadores de exposición a contaminantes en tres especies de bagres colombianos (Pisces: Siluriformes). *Biota Colombiana, 15*(1), 40–51.

González-Doncel, M., González, L., Fernández-Torija, C., Navas, J. M., & Tarazona, J. V. (2008). Toxic effects of an oil spill on fish early life stages may not be exclusively associated to PAHs: Studies with Prestige oil and medaka (*Oryzias latipes*). *Aquatic Toxicology, 87*(4), 280–288. https://doi.org/10.1016/j.aquatox.2008.02.013

Hansen, A., & Zielinski, B. S. (2005). Diversity in the olfactory epithelium of bony fishes: Development, lamellar arrangement, sensory neuron cell types and transduction components. *Journal of Neurocytology, 34*(3), 183–208. https://doi.org/10.1007/s11068-005-8353-1

He, T., Xiao, Z. Z., Liu, Q. H., Ma, D. Y., Xu, S. H., Xiao, Y. S., & Li, J. (2011). Stages of rock bream *Oplegnathus fasciatus* (Temminck & Schlegel, 1844): Embryonic development. *Aquaculture Research, 42*(12), 1764–1777. https://doi.org/10.1111/j.1365-2109.2010.02774.x

Holdridge, L. R., & Tosi Jr., J. A. (1967). *Life zone ecology*. Tropical Science Center. https://wiki.neotropicos.org/images/8/8e/LR_Holdridge_1966_life_zone_ecology.pdf

Honji, R. M., Tolussi, C. E., Mello, P. H., Caneppele, D., & Moreira, R. G. (2012). Embryonic development and larval stages of *Steindachneridion parahybae* (Siluriformes: Pimelodidae): Implications for the conservation and rearing of this endangered Neotropical species. *Neotropical Ichthyology, 10*, 313–327. https://doi.org/10.1590/S1679-62252012005000009

Kimmel, C. B., Ballard, W. W., Kimmel, S. R., Ullmann, B., & Schilling, T. F. (1995). Stages of embryonic development of the zebrafish. *Developmental Dynamics, 203*(3), 253–310. https://doi.org/10.1002/aja.1002030302

Kondakova, E. A., & Efremov, V. I. (2014). Morphofunctional transformations of the yolk syncytial layer during zebrafish development. *Journal of Morphology, 275*(2), 206–216. https://doi.org/10.1002/jmor.20209

Kossowski, C., & Madrid, F. (1991). Observaciones de los estadios embrionario y larval del bagre rayado cabezón *Pseudoplatystoma fasciatum* (Linnaeus, 1766) (Pisces, Siluriformes). *Biollania, 8*, 9–15.

Kozarić, Z., Kuzir, S., Petrinec, Z., Gjurcević, E., & Bozić, M. (2008). The development of the digestive tract in larval European catfish (*Silurus glanis* L.). *Anatomia, Histologia, Embryologia, 37*(2), 141–146. https://doi.org/10.1111/j.1439-0264.2007.00812.x

Landines, M. A., Senhorini, J. A., Sanabria, A. I., & Urbinati, E. C. (2003). Desenvolvimento embrionário do pintado (*Pseudoplatystoma coruscans* Agassiz, 1829). *Boletim Técnico do CEPTA, 16*, 1–13.

Lasso, C. A., Agudelo Córdoba, E., Luz, J. S., Ramírez-Gil, H., Morales-Betancourt, M. A., Ajiaco-Martínez, R. E., Gutiérrez, F. de P., Usma Oviedo, J. S., Muñoz Torres, S. E., Sanabria Ochoa, A. I., & Instituto de Investigación de Recursos Biológicos Alexander von Humboldt (Eds.). (2011). *Catálogo de los recursos pesqueros continentales de Colombia*. Instituto de Investigación de Recursos Biológicos Alexander von Humboldt.

Lemes, A. da S., & Braccini, M. del C. (2004). Descrição e análise histológica das glândulas anexas do trato digestório de *Hoplias malabaricus* (Bloch, 1794), (Teleostei, Erythrinidae). *Biodiversidade Pampeana*, *2*(1). https://revistaseletronicas.pucrs.br/biodiversidadepampeana/article/view/2530

Lencer, E. S., & McCune, A. R. (2018). An embryonic staging series up to hatching for *Cyprinodon variegatus*: An emerging fish model for developmental, evolutionary, and ecological research. *Journal of Morphology, 279*(11), 1550–1565. https://doi.org/10.1002/jmor.20870

Londoño, C., & Hurtado Giraldo, H. (2010). Estudio preliminar morfológico y morfométrico del encéfalo del pez tiburoncito *Ariopsis seemanni* (Pisces: Ariidae). *Universitas Scientiarum, 15*(2), 101–109.

Luz, R. K., Reynalte-Tataje, D. A., Ferreira, A. A., & Zaniboni-Filho, E. (2001). Desenvolvimento embrionário e estágios larvais do mandi-amarelo *Pimelodus maculatus*. *Boletim do Instituto de Pesca, 27*(1), 1–12.

Maldonado-Ocampo, J. A., Ortega-Lara, A., Usma Oviedo, J. S., & Calle, V. J. C. (Eds.). (2005). *Peces de los Andes de Colombia: Guía de campo*. Instituto de Investigación de Recursos Biológicos Alexander von Humboldt.

Martín, G. S., & Aguado, M. T. (2012). Contribution of scanning electron microscope to the study of morphology, biology, reproduction, and phylogeny of the family Syllidae (Polychaeta). In *Scanning electron microscopy*. IntechOpen. https://doi.org/10.5772/34681

Marques, C., Faustino, F., Bertolucci, B., Paes, M. do C. F., Silva, R. C. da, & Nakaghi, L. S. O. (2017). Embryonic development in *Zungaro jahu*. *Zygote*, *25*(1), 17–31. https://doi.org/10.1017/S0967199416000277

Marques, C., Nakaghi, L. S. O., Faustino, F., Ganeco, L. N., & Senhorini, J. A. (2008). Observation of the embryonic development in *Pseudoplatystoma coruscans* (Siluriformes: Pimelodidae) under light and scanning electron microscopy. *Zygote*, *16*(4), 333–342. https://doi.org/10.1017/S0967199408004838

Mojica, J. I., Usma Oviedo, J. S., Álvarez-León, R., & Lasso, C. A. (Eds.). (2012). *Libro rojo de peces dulceacuícolas de Colombia.* Instituto de Investigación de Recursos Biológicos Alexander von Humboldt. http://repository.humboldt.org.co/handle/20.500.11761/34197

Mojica, J. I., Galvis, G., Sánchez-Duarte, P., Castellanos, C., & Villa-Navarro, F. A. (2006). Peces del valle medio del río Magdalena, Colombia. *Biota Colombiana, 7*(1), 23–37.

Moncaleano, E., Sánchez, C., & Prieto Mojica, C. (2018). Estudio histológico y morfológico del desarrollo embrionario del pez capitán de la sabana (*Eremophilus mutisii*). *Revista U.D.C.A Actualidad & Divulgación Científica, 21*(2). https://doi.org/10.31910/rudca.v21.n2.2018.1073

Moreno, J. M., Aguilar, F. A., Boada, N. S., Rojas, J. A., & Prieto, C. (2019). Análisis morfométrico e índices corporales del capitán de la sabana. *Revista de la Facultad de Medicina Veterinaria y de Zootecnia, 66*(2), 141–153.

Morrison, C. M., Miyake, T., & Wright Jr., J. R. (2001). Histological study of the development of the embryo and early larva of *Oreochromis niloticus* (Pisces: Cichlidae). *Journal of Morphology, 247*(2), 172–195. https://doi.org/10.1002/1097-4687(200102)247:2<172::AID-JMOR1011>3.0.CO;2-H

Nakatani, K. (2001). *Ovos e larvas de peixes de água doce: Desenvolvimento e manual de identificação*. https://cir.nii.ac.jp/crid/1130571381504560668

Ninhaus-Silveira, A., Foresti, F., & de Azevedo, A. (2006). Structural and ultrastructural analysis of embryonic development of *Prochilodus lineatus* (Valenciennes, 1836) (Characiformes; Prochilodontidae). *Zygote, 14*(3), 1–10. https://doi.org/10.1017/S096719940600373X

Nogueira, L. B., Azevedo, P. G., Canelhas, M. R., Bedore, A. G., Lopes, J. M., & Godinho, H. P. (2012). Induced spawning and early ontogeny in hatchery-reared catfish *Zungaro jahu* (Siluriformes: Pimelodidae). *Neotropical Ichthyology, 10*(1), 89–98. https://doi.org/10.1590/S1679-62252012000100009

Novoa, J. D., & Cataño-Vergara, Y. M. (2005). *Descripción del desarrollo embrionario y larvario del blanquillo* (Sorubim cuspicaudus) [Trabajo de grado, Universidad de Córdoba].

Observatorio Español de Acuicultura. (2018). *Caracterización de la cría en cautividad y repoblación de especies de interés a través de la acuicultura*. https://observatorio-acuicultura.es/sites/default/files/images/adjuntos/libros/caracterizacion_cria_cautividad_repoblacion_especies_interes_14052018.pdf

Oliveira-Almeida, I. R., Buzollo, H., Costa, R. da S., Veríssimo-Silveira, R., Porto-Foresti, F., & Ninhaus-Silveira, A. (2015). Structural analysis of embryogenesis of *Leiarius marmoratus* (Siluriformes: Pimelodidae). *Zygote, 23*(5), 742–757. https://doi.org/10.1017/S0967199414000392

Ortega-Lara, A., Usma, J. S., Bonilla, P. A., & Santos, N. L. (2006). Peces de la cuenca alta del río Cauca, Colombia. *Biota Colombiana, 7*(1), 1–20. https://revistas.humboldt.org.co/index.php/biota/article/view/164

Portella, M. C., Jomori, R. K., Leitão, N. J., Menossi, O. C. C., Freitas, T. M., Kojima, J. T., Lopes, T. S., Clavijo-Ayala, J. A., & Carneiro, D. J. (2014). Larval development of indigenous South American freshwater fish species, with particular reference to pacu (*Piaractus mesopotamicus*): A review. *Aquaculture, 432*, 402–417. https://doi.org/10.1016/j.aquaculture.2014.04.032

Pradhan, P. K., Jena, J., Mitra, G., Sood, N., & Gisbert, E. (2013). Ontogeny of the digestive enzymes in butter catfish *Ompok bimaculatus* (Bloch) larvae. *Aquaculture, 372–375*, 62–69. https://doi.org/10.1016/j.aquaculture.2012.10.024

Prieto G. M., & Atencio, G. V. (2008). Zooplancton en la larvicultura de peces neotropicales. *Revista MVZ Córdoba, 13*(2), 1–10.

Puley, M., & Charles, A. (2022). Dissecting co-management: Fisher participation across management components and implications for governance. *Fish and Fisheries, 23*(3), 719–732. https://doi.org/10.1111/faf.12645

Ramírez-Merlano, J. A., Otero-Paternina, A. M., Corredor-Santamaría, W., Medina-Robles, V. M., Cruz-Casallas, P. E., & Velasco-Santamaría, Y. M. (2010). Utilización de organismos vivos como primera alimentación de larvas de yaque (*Leiarius marmoratus*) bajo condiciones de laboratorio. *Orinoquia, 14*(1), 45–58.

Riveros-Pinilla, D. A., Ramírez-Merlano, J. A., Sandoval-Vargas, L. Y., Mira-López, T. M., Cruz-Casallas, P. E., & Medina-Robles, V. M. (2017). Efecto del protocolo de inducción hormonal en la espermiación y las características seminales de yaque (*Leiarius marmoratus*). *Orinoquia, 21*(1), 34–40. https://doi.org/10.22579/20112629.392

Rodrigues-Galdino, A. M., Maiolino, C. V., Forgati, M., Donatti, L., Mikos, J. D., Carneiro, P. C. F., & Rios, F. S. (2010). Development of the neotropical catfish *Rhamdia quelen* (Siluriformes: Heptapteridae) incubated in different temperature regimes. *Zygote, 18*(2), 131–144. https://doi.org/10.1017/S096719940999013X

Rosas, J., Mata, E., Velásquez, A., & Cabrera, T. (2008). Desarrollo embrionario-larval del pez tropical *Hemirhamphus brasiliensis* (Beloniformes: Hemirhamphidae) a partir de huevos recolectados del medio natural. *Revista de Biología Tropical, 56*(3), 1449–1458.

Rønnestad, I., Yúfera, M., Ueberschär, B., Ribeiro, L., Sæle, Ø., & Boglione, C. (2013). Feeding behaviour and digestive physiology in larval fish: Current knowledge, and gaps and bottlenecks in research. *Reviews in Aquaculture, 5*(Suppl. 1), S59–S98. https://doi.org/10.1111/raq.12010

Sato, Y. (1999). *Reprodução de peixes da bacia do rio São Francisco: Indução e caracterização de padrões* [Tese de doutorado, Universidade Federal de São Carlos].

Steindachner, F. (1879). Über einige neue und seltene Fischarten aus den zoologischen Museen zu Wien, Stuttgart und Warschau. *Anzeiger der Kaiserlichen Akademie der Wissenschaften, Mathematisch-Naturwissenschaftliche Classe*, *16*, 29–34.

Valbuena-Villarreal, R. D., Zapata-Berruecos, B. E., David-Ruales, C., & Cruz-Casallas, P. E. (2012). Desarrollo embrionario del capaz *Pimelodus grosskopfii* (Steindachner, 1879). *International Journal of Morphology, 30*(1), 1–10. https://doi.org/10.4067/S0717-95022012000100027

Vazzoler, A. E. A. de M. (1996). *Biologia da reprodução de peixes teleósteos: Teoria e prática*. EDUEM.

Villa-Navarro, F. A., Acero, A., & Cala, P. (2017). Taxonomic review of Trans-Andean species of *Pimelodus* (Siluriformes: Pimelodidae), with the description of two new species. *Zootaxa, 4299*(3), 337–360.

Villa-Navarro, F. A., Usma-Oviedo, J. S., Mesa-Salazar, L., & Sánchez-Duarte, P. (2016). *Pimelodus grosskopfii*. In *The IUCN Red List of Threatened Species* (2016:

e.T49829828A61473588). https://www.iucnredlist.org/species/49829828/61473588

Yepes-Blandón, J. A., Vásquez-Machado, G., Ávila-Coy, J., Ortiz-Acevedo, Y., & Estrada-Posada, A. (2022). Embryogenesis and early larval development in bocachico (*Prochilodus magdalenae*) in Colombia. *The Journal of Basic and Applied Zoology, 83*(1), 58. https://doi.org/10.1186/s41936-022-00299-2

Yúfera, M., & Darias, M. J. (2007). The onset of exogenous feeding in marine fish larvae. *Aquaculture, 268*(1), 53–63. https://doi.org/10.1016/j.aquaculture.2007.04.050

Zadmajid, V., Mirzaee, R., Hoseinpour, H., Vahedi, N., & Butts, I. A. E. (2017). Hormonal induction of ovulation using Ovaprim™ [(D-Arg6, Pro9NEt)-sGnRH + domperidone] and its impact on embryonic development of wild-caught longspine scraper *Capoeta trutta* (Heckel, 1843). *Animal Reproduction Science, 187*, 79–90. https://doi.org/10.1016/j.anireprosci.2017.10.009

Zadmajid, V., Sørensen, S. R., & Butts, I. A. E. (2019). Embryogenesis and early larval development in wild-caught Levantine scraper *Capoeta damascina* (Valenciennes, 1842). *Journal of Morphology, 280*(1), 1. https://doi.org/10.1002/jmor.20926

Zavala-Leal, I., Dumas-Lapage, S., & Peña-Martínez, R. (2011). Organogenesis during the larval period in fishes. *CICIMAR Oceánides, 26*(2), 19–30. https://doi.org/10.37543/oceanides.v26i2.100

Zeng, C., Liu, B. S., Zhu, K. C., Guo, H. Y., Guo, L., Zhang, N., Liu, B., Wang, Z. Y., & Zhang, D. C. (2020). Histological study on the development of the digestive system of the longfin batfish (Platax teira). *Israeli Journal of Aquaculture – Bamidgeh, 72*, 21466. https://doi.org/10.46989/001c.21466